Controlling Order in Block Copolymer Thin Films for Nanopatterning Applications

Andrew P. Marencic and Richard A. Register

Department of Chemical and Biological Engineering, Princeton University, Princeton, New Jersey 08544; email: register@princeton.edu

Annu. Rev. Chem. Biomol. Eng. 2010. 1:277–97

First published online as a Review in Advance on February 26, 2010

The *Annual Review of Chemical and Biomolecular Engineering* is online at chembioeng.annualreviews.org

This article's doi:
10.1146/annurev-chembioeng-073009-101007

1947-5438/10/0715-0277$20.00

Key Words

alignment, surface energy, topological defect, orientational order, translational order, substrate

Abstract

An attractive "unconventional" lithographic technique to pattern periodic, sub-100 nm features uses self-assembled block copolymer thin films as etch masks. Unfortunately, as-cast films lack the orientational and positional order of the microphase-separated domains that are necessary for many desired applications. Reviewed herein are techniques developed to guide the self-assembly process in thin films, which permit varying degrees of control over the patterns formed by the microdomains. Techniques that can control the out-of-plane order of the microdomains are first summarized. Then, techniques that control the lateral ordering are reviewed, beginning with those that generate large defect-free grains, then those that impart orientational order to the microdomains, and finally those that can control both the orientation and position of individual microdomains. Each technique is summarized with experimental examples and discussions regarding the mechanism of the guided self-assembly process.

INTRODUCTION

With the continued miniaturization of microfabricated structures reaching the photolithographic limit of ~100 nm, alternative methods of creating high-resolution patterns on even smaller length scales are highly desired. The utilization of self-assembled materials, particularly block copolymers in thin films, is one avenue to follow because block copolymers spontaneously form periodic "microdomain" structures of various symmetries (**Figure 1**) on the scale of tens of nanometers, with the microdomain size and periodicity tunable by adjusting the molecular weights of the individual blocks (1, 2). Thin films containing these microdomain structures can then be used as nanolithographic etch masks to create dot or line patterns on solid surfaces (3–8). Block copolymer nanopatterning has already demonstrated its usefulness by creating nanowire polarizer grids (9, 10), high-density arrays of cobalt nanowires oriented perpendicular to the substrate (11), metal nanodot (12) and nanopore arrays (13), and patterned magnetic media (14), to name a few of the many examples. Other applications of block copolymer thin films include creating nanoporous materials (15, 16) as templates to incorporate nanoparticles (17) or biomolecules (18) and as switchable smart surfaces (19).

Many of the applications listed above require precise control of the microdomain order such that the line or dot structures are free from topological defects that destroy the translational and/or orientational order. Much work has been done in tackling this problem using many different techniques, each with its own benefits and drawbacks. This article reviews the different techniques used to control the block copolymer microdomain orientation and order in thin films. It begins by describing phase separation and morphology in block copolymers and the effects that confinement has on these aspects when the copolymers are in thin films. Next, techniques used to orient microdomains normal to the surface will be reviewed. Control of the in-plane structures will be covered in the rest of the review, beginning with techniques to generate large-area, defect-free patterns, followed by techniques that yield long-range orientational order, and finishing with techniques that also control the positional order of the microdomains.

SELF-ASSEMBLY IN BULK

Phase separation between two species occurs when the magnitude of the enthalpic contribution (usually positive and decreasing with temperature) to the free energy of mixing the two components is greater than the magnitude of the entropic contribution (always negative and ideally temperature-independent); phase separation thus minimizes unfavorable interactions between dissimilar species. For a mixture of two or more polymers, the entropic contribution is severely reduced because the covalent bonds prohibit the monomer units from independently sampling the whole space, thus enhancing the tendency for phase separation; however, in block copolymers, the covalent bonds between blocks preclude their macroscopic phase separation. The equilibrium structure will minimize the interactions between the dissimilar blocks while still avoiding overstretching of the polymer chains (20). For a diblock copolymer with blocks of near-equal length, the blocks will separate into alternating lamellar structures. As one block becomes longer than the other, the interface begins to curve to maintain approximately equal stretching of the dissimilar blocks, and the morphology transitions to bicontinuous gyroidal, then hexagonally-packed cylindrical, and finally body-centered-cubic (*bcc*) packed spherical morphologies as the asymmetry increases (**Figure 1**) (21, 22). Allowing one or more of the blocks to be polydisperse can skew the phase diagram, widen the windows for certain phases, and even open coexistence regions between different ordered morphologies (23). Adjusting the architecture further to include linear ABC triblock copolymers (24), comb block copolymers (25), or dendritic copolymers (26) can yield a vast array of microphase-separated structures.

SELF-ASSEMBLY IN THIN FILMS

Confining the block copolymer to a thin film can impact the ordering and morphology via interactions with the confining surfaces. Each of the different surfaces (air and substrate) usually has a preferential affinity for one block in the copolymer, so typically that block will wet that particular surface; for morphologies having anisometric microdomains, such as cylinders and lamellae, these preferential surface interactions thereby induce the microdomains to lie parallel to the substrate (27, 28). For lamellae-forming diblock copolymer thin films, this results in a discretization of the film thickness at integer multiples of the interdomain spacing ($d = nL_0$, where d is the film thickness, n is an integer, and L_0 is the lamellar spacing) for symmetric wetting conditions (the same block wets both surfaces) and at half-integer thicknesses [$d = (n + 1/2)L_0$] for asymmetric wetting conditions. Islands or holes, collectively called terraces and resulting in surface topography, will form if the average film thickness is incommensurate with these values because the energetic penalty for creating more film surface area is less than the penalty caused by altering the domain periodicity (chain stretching or compression) or by putting an energetically disfavored block in contact with one or both surfaces (29, 30). If $d < L_0$, perpendicular morphologies are possible (31); these are discussed in the next section.

Cylinder-forming diblock copolymers behave similarly in that the affinity of one block for a surface will orient the cylinders parallel to the substrate. If a surface has a preferential affinity for the minority component, then a brush-like wetting layer typically forms, coating the entire surface with the minority block (32). Discretized film thicknesses are also observed in these thin films; however, interesting morphologies can form at the edges of the terraces, including perpendicularly oriented cylinders and perforated lamellar structures (33, 34). These transitions are also observed in ABA triblock copolymers (35–37). At certain thicknesses the cylindrical morphology will transition to a close-packed spherical morphology because of the high energy cost of distorting the cylinders away from their preferred spacing (38).

Sphere-forming diblock copolymers display similar behavior: Brush-like wetting layers can form (if the minority block wets the interface), and stacking of microdomain layers occurs (39). In bulk, the spheres pack into a *bcc* lattice, but in thin films, a monolayer of spheres packs into a close-packed configuration, which may be viewed as a distorted ⟨1 1 0⟩ plane of the *bcc* structure, as there are no longer any neighboring layers to break the in-plane symmetry. The transition from thin film packing to bulk packing was investigated for thin films of poly(styrene-*b*-2-vinylpyridine) (PS-*b*-P2VP); Stein et al. found a hexagonal close-packed (*hcp*) structure for up to three layers of spheres, then a face-centered orthorhombic (*fco*) phase that progressively changes its lattice parameters as the number of layers increases from 4 to 23, asymptotically approaching a ⟨1 1 0⟩ *bcc* structure (40, 41). The number of layers at which the *fco* structure becomes stable and the rate at which the *fco* structure approaches the bulk *bcc* packing are predicted to depend on the interblock segregation strength, with the *hcp* structure remaining stable for greater film thicknesses as segregation strength is reduced (40).

Adjustments to the size and/or spacing of the microdomains are possible by blending the block copolymer with its corresponding homopolymers. Mayes et al. showed that the domain spacing of a lamellae-forming poly(styrene-*b*-methyl methacrylate) (PS-*b*-PMMA) block copolymer thin film can be increased by adding the homopolymer of either block; the homopolymer increasingly prefers to reside at the domain center as its molecular weight increases (42). Similar results were found by Jeong et al. for the corresponding cylinder-forming block copolymer/homopolymer blends (43). Controlled domain size and spacing increases were also observed in symmetric ternary blends of PS-*b*-PMMA with its homopolymers for lamellae- (44) and cylinder-forming (45) block copolymer thin films.

CONTROLLING OUT-OF-PLANE ORIENTATION

A striped pattern in a thin film of a cylinder-forming block copolymer, or a dot pattern in a sphere-former, can be transferred into a substrate by etching; however, the aspect ratio of the features is limited because both domains are etched during processing. Orienting lamellae-forming block copolymers or cylinder-forming block copolymers perpendicular to the surface could enhance the aspect ratio of the features produced and eliminate the terracing induced by film quantization effects. When the dissimilar blocks show no preferential affinity for either surface, the microdomains prefer to orient perpendicular to the substrate to accommodate the necessary block stretching (46). Many different approaches have been used to neutralize the substrate surface. Peters et al. used self-assembled monolayers of octadecyltrichlorosilane (OTS) that were chemically altered by X rays in the presence of air to generate aldehyde and hydroxyl groups that, at the proper level, can yield a neutral surface for PS-*b*-PMMA (47). Grafting of random copolymers to surfaces can also balance the interactions between the dissimilar blocks and orient block copolymer microdomains perpendicular to the substrate (48–53). Mansky et al. found the optimal PS content (~60%) in a PS-*r*-PMMA copolymer to neutralize the surface for a lamellae-forming PS-*b*-PMMA (48, 49). Ham et al. later showed that the range of PS content in the random copolymer yielding perpendicular cylinders for PS-*b*-PMMA was slightly different than the range yielding perpendicular lamellae (50). Han et al. used varying substrate-modifying layers consisting of PS-*r*-PMMA and a third comonomer, either 2-hydroxyethyl methacrylate (HEMA, if grafting onto a silicon oxide surface) or glycidyl methacrylate (GMA, if crosslinking the random copolymer into a mat), to reorient lamellae-forming and cylinder-forming PS-*b*-PMMA (51). They found distinct windows for perpendicular orientations for the different combinations of random brushes and block copolymers, which showed that the equilibration of the block copolymer in the presence of the random brushes, and not just the interfacial energies of the blocks and brushes, must be considered. Ji et al. described a generalizable method that uses a ternary blend of functionalized homopolymers of A and B (which react with the substrate to form the brush) and a low-molecular-weight A-*b*-B diblock (used to homogenize the blend) to neutralize the surface (demonstrated using PS and PMMA) (52). Because many block copolymers have a larger surface energy difference between blocks than does PS-*b*-PMMA (in which the difference is close to zero at convenient annealing temperatures), work was done to verify that lamellae-forming PS-*b*-P2VP, which has a large surface energy difference between blocks, could be perpendicularly oriented on PS-*r*-P2VP-*r*-PHEMA (53). Perpendicular microdomain orientation will persist through relatively thick films only if both surfaces are closely neutral (54). Roughening the substrate can also induce reorientation because a penalty is incurred for elastic deformation to conform to a rough substrate (55). Sivaniah et al. observed perpendicular orientations in lamellae-forming PS-*b*-PMMA on a rough substrate (56), as did Maire et al. for cylinder-forming block copolymers (although not on all substrates tested) (57). Yager et al. were able to adjust the substrate roughness using silica nanoparticles to orient a lamellae-forming PS-*b*-PMMA block copolymer for certain film thicknesses (58). Chemically patterned surfaces have been generated that have periodic affinities to each block, which causes a lamellae-forming block copolymer to orient perpendicularly to the surface (59). Because of the precise control afforded by using this method, it will be covered in the subsequent section on controlling positional order.

Reorientation can also be achieved by incorporating additives into the block copolymer. Lin et al. added cadmium selenide nanoparticles to a cylinder-forming PS-*b*-P2VP block copolymer, which caused reorientation of the microdomains perpendicular to the substrate because the particles segregate at the interface and mediate the block copolymer/substrate interactions (60). A cylinder-forming blend of PS-*b*-PMMA with poly(ethylene

oxide)-coated gold nanoparticles (Au-PEO) can be induced to orient perpendicular to the substrate by annealing in humid air (61). Addition of homopolymer to a block copolymer thin film not only adjusts the domain spacing and/or size but can also reorient the microdomains. Jeong et al. showed that addition of dry-brush PMMA homopolymer to a cylinder-forming PS-*b*-PMMA block copolymer will stabilize the perpendicular orientation of the microdomains in thicker films (hundreds of nanometers) (62). Wang et al. induced a perpendicular orientation of a lamellae-forming block copolymer by adding lithium chloride to PS-*b*-PMMA (63). They observed orientations of the lamellae normal to the surface when ~20% of the carbonyl groups were complexed with lithium ions. Incorporation of a low surface energy midblock—which creates a triblock copolymer—can also induce a perpendicular orientation through the entropic penalty for looping the midblock, which is required for a parallel orientation. Khanna et al. showed that lamellae- and cylinder-forming poly(cyclohexylethylene-*b*-ethylene-*b*-cyclohexylethylene) (PCHE-*b*-PE-*b*-PCHE) triblocks orient perpendicular to the substrate, whereas a PCHE-*b*-poly(ethylene-*r*-butylene)-*b*-PCHE (PCHE-*b*-PEB-*b*-PCHE) block copolymer remained parallel to the substrate, which demonstrated that the difference in surface energies between the blocks must be small for midblock looping to dominate the energetics (64). Kubo et al. showed similar results for a cylinder-forming PS-*b*-poly(isoprene)-*b*-poly(lactide) (PS-*b*-PI-*b*-PLA) (65).

External forces have also been used to overcome surface forces and orient block copolymer microdomains perpendicular to the substrate. Thurn-Albrecht et al. have demonstrated the use of electric fields in orienting cylinder-forming PS-*b*-PMMA block copolymers perpendicular to the substrate, as sufficient contrast in dielectric permittivity exists between these two blocks (66). They applied a voltage across the thin film by sandwiching the block copolymer between two aluminum electrodes with a Kapton spacer to avoid shorting. They determined the minimum voltage necessary to overcome the surface energy difference and orient the microdomains normal to the surface, independent of film thickness (up to 30 μm). If annealed from the disordered state, the electric field orients concentration fluctuations that form into oriented cylinders as the temperature is decreased (67). From a microphase-separated parallel orientation, the electric field causes the cylinders to break up into spheres, which then reconnect to form cylinders that tilt toward the electric field orientation with continued annealing (68). Xu et al. were able to align lamellae-forming PS-*b*-PMMA with an electric field, although not for all thicknesses (thin films stubbornly remained parallel, whereas very thick films, $>10L_0$, had parallel orientations near their surfaces) (69). They determined that defect movement and coalescence is the main mechanism by which reorientation occurs. Voicu et al. used a combination of bottom-up and top-down approaches based on electrohydrodynamic formation of surface patterns to orient lamellae-forming PS-*b*-PMMA (70). An array of pillars of the block copolymer form when electrostatic pressure overcomes the surface tension of the polymer-air interface, and a perpendicular domain orientation is induced by the combination of flow during the pillar formation and interaction with the electric field (**Figure 2**). Solvent casting the block copolymer thin film from a preferential solvent has been shown to orient the microdomains perpendicular to the substrate because the evaporation of the solvent is highly directional (71). Because solvent also imparts enhanced mobility into the block copolymer chains and accelerates grain growth, its use will be covered in the next section.

GENERATION OF LARGE GRAINS

For nanopatterning applications, researchers would like to be able to easily control the 2D in-plane order of the block copolymer film. As-cast thin films are rife with topological defects (**Figure 3**) that

quickly destroy the orientational and translational order because grains nucleate independently and in random orientations throughout the sample. Thermally annealing the film above the glass transition temperature imparts mobility to the block copolymer chains such that the energetically unfavorable defects (whose strain field causes nonuniform chain stretching) will annihilate. Harrison et al. followed the dynamics of defect movement and annihilation using cylinder-forming (72, 73) and sphere-forming (74) PS-*b*-poly(ethylene-*alt*-propylene) (PS-*b*-PEP) block copolymers and showed that the orientational correlation length ξ increases with a weak power in time ($\xi \sim t^{1/4}$). For the cylinder-former, they observed coherent annihilation of disclination quadrupoles as the primary means of increasing the orientational correlation length. For the sphere-former, they observed few disclinations, but the dislocations present (mostly found along grain boundaries) were progressively annihilated during grain shrinkage, which most frequently occurs when a small grain is absorbed by two adjacent, larger grains. Horvat et al. observed modifications of the classical structures at defect sites, such as perforated lamellae and necks connecting the cylinders of a PS-*b*-poly(butadiene) (PS-*b*-PB) block copolymer, which should enhance the chain mobility by interconnecting the minority component domains (75).

It is apparent that thermal annealing is not a practical avenue to eliminate the topological defects and create global long-range order in these materials. Angelescu et al. showed that larger grains with fewer defects (no disclinations and an order of magnitude reduction in the number of dislocations) can be obtained using a solidification front sweeping across the order-disorder temperature for cylinder-forming PS-*b*-PEP (76). A more robust technique, which does not require a thermally accessible order-disorder transition, uses solvent fields. The presence of solvent in the block copolymer can perform several functions simultaneously: It can mediate surface energies, create an ordering front as the solvent directionally evaporates, and impart mobility to the film without elevated temperatures (71). Kim et al. observed that the orientation of a cylinder-forming PS-*b*-PB-*b*-PS thin film is a function of evaporation rate, with perpendicular orientation achieved for fast rates (77). Lin et al. showed the same effect for cylinder-forming PS-*b*-PEO and attributed the orientation to a moving gradient of solvent concentration normal to the surface, which creates an ordering front that propagates from the air surface into the film (78). These films contained a large number of defects in the hexagonal in-plane lattice, which could be eliminated by annealing in the vapor of a good solvent for both blocks (79). Nearly defect-free arrays of perpendicular cylinders in PS-*b*-poly(4-vinylpyridine) (PS-*b*-P4VP) were also created after annealing in tetrahydrofuran vapor (71). Selective solvents could be used to swell one of the blocks, possibly enough to alter the morphology from its equilibrium structure. Chen et al. used acetone as a selective solvent for PMMA in a PS-*b*-PMMA diblock and observed spherical morphologies initially and then cylindrical and lamellar morphologies after continued annealing (80). These morphologies can be frozen in place because both blocks vitrify at room temperature after removal of the solvent.

CONTROLLING IN-PLANE ORIENTATION

Whereas large, defect-free grains can be generated using thermal or solvent annealing, the methods discussed above yield no preferred orientation for the grains. However, control over the in-plane directionality of the microdomains is desired for many applications. A variation of the sweeping temperature front discussed above (76) was developed by Berry et al. to preferentially orient cylinder-forming PS-*b*-PMMA in the direction of the front motion (81). Here the temperature is kept below the order-disorder temperature but crosses the glass transition temperature of the block copolymer. They created their temperature gradient by passing the sample (at a controllable rate) across a hot block between two cold blocks, which creates a bell-shaped temperature profile for each spot in the film as a function of time. They observed more rapid defect motion and increased

orientation as the velocity of the sample decreased. They attribute the ordering to the creation of an in-plane spatiotemporal mobility gradient that biases the grains as they form. Self-consistent field theory (SCFT) calculations on striped patterns within a spatiotemporally heterogeneous mobility field showed that a mobility gradient can be useful as a means of controlling microdomain order with respect to the annealing direction (82).

A thickness gradient can impart lateral control over the orientation of perpendicular lamellae in block copolymer thin films. Kim et al. used film dewetting to create perpendicular PS-*b*-PMMA lamellae on a neutral surface that spontaneously align along the thickness gradient (83). Later they also used drop casting and thermal imprinting to create controlled thickness gradients and to investigate the mechanism more fully (84). They determined the underlying mechanism to be geometric anchoring caused by the tilted top surface. This tilt creates an elastic penalty for any orientation of the lamellae other than along the thickness gradient. This elastic penalty, in conjunction with the preferential movement of defects from the thicker part of the film to the thinner part, produces alignment (**Figure 4**).

Casting lamellae-forming block copolymers on corrugated substrates can have a similar effect. Kim et al. used electron-beam (e-beam) lithography to create a prepatterned substrate with a feature height comparable with the thickness of the film. They then cast a lamellae-forming blend of PS-*b*-PEO with polymethylsiloxane resin (PS-*b*-PEO/PMS) on this neutralized surface (85). The lamellae orient perpendicular to the direction of the corrugation because the energy cost for distortion of the polymer chains causes them to follow the contour of the surface structure. Later, the authors used lamellae-forming PS-*b*-PMMA to determine the effects of the periodicity of the features and of the ratio of feature height to film thickness, and found a narrow window for lateral alignment (86). Park et al. used surface-reconstructed sapphire wafers to orient perpendicular cylinder-forming PS-*b*-PEO block copolymers along the sawtoothed substrate topography after solvent annealing (**Figure 5**) (87). They observed excellent registry of the block copolymer with the topography and even defect tolerance, in that dislocations in the faceted surface did not propagate into dislocations in the block copolymer lattice.

As discussed previously, electric fields can be used to orient block copolymer thin films perpendicular to the substrate. In-plane orientation of block copolymer thin films can also be controlled using electric fields if electrodes are placed on the substrate. Morkved et al. demonstrated that the cylinders in asymmetric PS-*b*-PMMA will align their axes with the electric field lines for fields >30 kV cm^{-1}, even when the field lines are curved (88). Mansky et al. scaled up this technique to produce alignment of the cylindrical microdomains with the electric field over an area of 2 cm^2 (89). They lithographically created interdigitated electrodes (1000 lines separated by 12 μm each from two electrodes) to generate the required electric field strength.

Flow fields are also highly effective in orienting block copolymer microdomains. Albalak et al. used roll-casting, wherein a block copolymer solution is allowed to evaporate while an extensional flow is induced between two corotating rolls to orient cylinders and lamellae parallel to the extension direction (90). Although this process produces only thick films (down to 50 μm), other flow alignment techniques are possible on thin films. Kimura et al. used the flow of a droplet pinned to a tilted surface in conjunction with solvent evaporation to orient a cylinder-forming PS-*b*-PB thin film (91). The pinning of the drop causes directional flow within the droplet normal to the pinned edge, which induces ordering as the solvent evaporates. Angelescu et al. were able to orient a monolayer of cylinder-forming (92) and a bilayer of sphere-forming (93) PS-*b*-PEP using a crosslinked poly(dimethylsiloxane) (PDMS) pad pulled laterally over the surface. This process could quickly (∼30 minutes) orient the microdomains over large areas (∼1 cm^2). Later, Wu et al. and Pelletier et al. showed that alignment can also be achieved by flowing a viscous fluid over the block copolymer thin film (94, 95). They observed that above a certain stress, macroscopic

orientational order in these thin films is achieved (orientational correlation persists over the entire sheared area), though residual dislocations still limit the translational order (96). Alignment of the film in this process was proposed to proceed through a preferential "melting" of the grains most misaligned with the shear direction followed by microdomain reformation in the correct orientation. Further tests were conducted on this proposed mechanism by shearing the samples a second time, which essentially adjusted the initial condition from a polygrain state to a monograin state (97). Here the cylinder-forming block copolymers quantitatively conformed to the model, but the sphere-formers required a larger stress than expected, which was attributed to the need to nucleate a "molten" region so that shear-alignment can proceed. Computer simulations on cylindrical micelles verified this proposed mechanism (98), but simulations on a bilayer film of the spherical phase did not reveal microdomain melting/reformation (99). Instead, spheres in the two layers adjusted their positions to minimize frictional drag between the two layers, causing the spheres to move in a zigzag pattern. Another mechanism is possible if the sphere-forming block copolymer is close to the sphere/cylinder phase boundary: The shear can cause the spheres to transform into cylinders, which orient with the shear. Hong et al. observed this phenomenon in both single-layer and bilayer films of a sphere-forming PS-*b*-PI (100).

Polarized light has been used to orient specially-designed liquid crystalline PEO-*b*-poly(methacrylate-azobenzene) diblocks (PEO-*b*-PMA/AZ) in multilayer films, though not yet in the single-layer films desired for nanopatterning. Yu et al. showed that as-cast films had PEO cylinders oriented perpendicular to the substrate, but upon irradiation, the cylinders orient parallel to the surface and perpendicular to the polarization direction of the laser light (**Figure 6**) (101). Morikawa et al. were able to tailor the orientation of the block copolymer either parallel or perpendicular to the substrate by adjusting the film thickness and then to orient in-plane cylinders using holographic laser irradiation (102). The AZ moiety orients perpendicular to the polarization of the laser light by repetition of the *trans-cis-trans* isomerization cycle, with supramolecular cooperative motion transferring such ordering to the other block. Later, Morikawa and coworkers were able to use photoinduced alignment on PS-*b*-PMA/AZ, a block copolymer with a higher glass transition temperature (103).

Epitaxial crystallization can be used to control the chain orientation of semicrystalline block copolymer thin films. De Rosa et al. used the surface interaction due to crystallographic matching of atomic-scale unit cells between a semicrystalline lamellae-forming PE-*b*-PEP-*b*-PE (PE = crystalline polyethylene) and crystalline benzoic acid (BA) to induce lamellae oriented perpendicular to the surface with the *c* axis of the PE crystallites parallel to the *a* axis of the BA crystal (104). The authors induced directional crystallization of BA to create large ⟨0 0 1⟩ surfaces that the PE component could crystallize onto. Later they used the same technique to orient a cylinder-forming PS-*b*-PE perpendicular to the substrate with pseudohexagonal packing of the cylinders in the direction of the *b* axis of the BA (105). The stretched hexagonal lattice is caused by the transformation from unstable lamellae to cylinders during the crystallization of the block copolymer. The researchers also were able to use this process to orient noncrystalline block copolymers (106, 107). Lamellae-forming PS-*b*-PMMA oriented perpendicular to the substrate and along the *b* axis of the templating crystal, and cylinder-forming PS-*b*-PI oriented either parallel to the substrate, with the cylinders oriented along the *b* axis of the templating crystal, or perpendicular to the substrate, with the nearly hexagonal lattice along the *b* axis, depending on film thickness.

CONTROLLING IN-PLANE POSITIONAL ORDER

Although the previous section outlined several techniques for orienting the microdomains in a particular direction, often over large areas (on the order of square centimeters), such films still

contain residual defects that limit the translational order to short range. Striped patterns contain breaks that would limit their use as masks to create nanowires for applications in which continuity is necessary, whereas dot patterns contain dislocations that would limit their use as masks to create data storage arrays that require perfect placement of the features. Discussed below are techniques that potentially allow complete control over the placement and sometimes the shape of the block copolymer microdomains.

Graphoepitaxy utilizes the topography of the substrate, which can have a length scale many times the repeat spacing of the block copolymer, to control the in-plane orientation of the microdomains. Segalman et al. oriented sphere-forming PS-*b*-P2VP into single grains by prepatterning a surface with topographic relief structures that are spaced by 4.5 μm and are approximately one domain spacing tall (108). Within the troughs, the spheres orient a line of spheres parallel to the confining wall, but on top of the mesas, the lines of spheres make a ~5° angle with the edge. The order persists from the wall outward, but is limited by the dynamics of coarsening (74) such that a single grain of spheres could be created only when the trough/mesa was <5 μm in width. The authors also observed the creation of a grain boundary when a corner of a relief structure was not commensurate with the angle dictated by the hexagonal lattice (≠60°, 120°) (109). Cheng and coworkers extended this idea to investigate the effect that channel width and line edge roughness have on the ordering of a monolayer of sphere-forming PS-*b*-poly(ferrocenyldimethylsilane) (PS-*b*-PFS) (110–114). They observed single-grain structures within troughs containing 1–12 rows of spheres, but not more (110–112). By gradually adjusting the trough width, they were able to observe stretching of the microdomain spacing perpendicular to the trough edges (111, 112). In very narrow troughs that can accommodate only one line of spheres, if the width does not match the domain spacing, the spheres deform into ellipsoids (113). Large-wavelength undulations in the sidewalls alter the local width of the trough so that the number of rows of spheres can vary along the trough length, with dislocations present where the number of rows changes (111, 112). Some control over translational order can be imparted to the sphere array by placing a point defect, with a size comparable with that of a microdomain, along the sidewall such that the spheres then form a monodomain with the defect incorporated into the lattice (111). Easier still would be to use a 2D template with a sharp 60° corner (114). Hexemer et al. and Stein et al. demonstrated such orientation for PS-*b*-P2VP confined within a hexagonal well with 120° corners (115–117). They observed single-grain structures for hexagons up to 12 μm across, with very few if any dislocations observed in certain sizes of wells (115). Although the orientational order of the spheres within a 12-μm-wide hexagonal well spanned the width of the well, the translational order decayed with distance (116, 117), which limits the use of graphoepitaxy for precise control of translational order unless the features that control positional order (60° or 120° corners or point defects) are close together. Using SCFT, Bosse et al. simulated the packing of spheres within a hexagon having a side only five microdomain spacings long and analyzed the effects that wetting conditions, surface roughness, and small changes in well size have on the ordering and occurrence of defects (118). Later Hur et al. used SCFT to simulate the packing of a block copolymer/homopolymer blend within a square well only four microdomain spacings wide (119). Adding homopolymer facilitated the adoption of square packing over a narrow range of well widths, which is particularly attractive because square packing is consistent with industry standard design architecture.

Graphoepitaxy can also be used to align striped patterns from cylinder- or lamellae-forming block copolymers. Sundrani et al. oriented cylinder-forming PS-*b*-PEP thin films within troughs with the cylinder axis parallel to the walls (120, 121). They investigated the ordering as a function of trough width and observed that dislocations formed when the width of the channel changed, requiring the addition or removal of a cylinder. They also created a +1/2 disclination as the cylinders followed the dome-shaped end of a trough. Park et al. were able to control the orientation

of a lamellae-forming PS-*b*-PMMA thin film using both topographic and chemical patterning (122). The lamellae could be oriented perpendicular to the substrate and along the confining edge provided that there was simultaneously a neutral PS-*r*-PMMA layer on the substrate surface and a surface preferential to one of the blocks on the confining edge. If all surfaces are neutral, then the lamellae preferentially orient perpendicular to both the substrate and confining wall. Sundrani & Sibener observed PS-*b*-PMMA cylinders with their axes perpendicular to the trough walls (123). In this case thicker films with islands and holes form on top of the topographic patterns; these terraces flow from the top of the mesas into the grooves such that the cylinders orient with the flow field, perpendicular to the trough walls. Park et al. created structures wherein PS-*b*-PMMA lamellae were simultaneously perpendicular to both the trough walls and the nonselective substrate (124). They were also able to achieve some translational order by controlling the registry of the lamellae by including a sharp step down at the end of the parallel ridges. More complex structures are also possible: Yamaguchi et al. used lamellae-forming PS-*b*-PMMA, which aligns with the topographical edge when neutral surfaces are present on the substrate only, to bend around a 90° corner or form concentric circles within small ($<6L_0$) hexagons (125). Jeong et al. were also able to generate concentric circles within a small ($6–7L_0$ in diameter) circular well formed in a strippable photoresist (126). A lamellae-forming blend of PS-*b*-PEO with low-molecular-weight organosilicate, which orients perpendicular to both the substrate and the topographical edge, was confined in designed geometries (90° bend, U-shape, rounded rectangle, and circle) to create complex patterns (127).

Because chemically altered surfaces can control microdomain orientation by spatially modulating the surface chemistry across the substrate, a different kind of graphoepitaxy can be achieved in which topographical features on the substrate are replaced by transitions in wetting behavior. Yang et al. used extreme UV interferometric lithography (EUV-IL) to alter the surface chemistry of OTS on the micron scale, then deposited lamellae-forming PS-*b*-PMMA on the chemically patterned OTS (128). The PS block wets the unexposed OTS whereas the PMMA block wets the exposed OTS, orienting the lamellar microstructure perpendicular to the substrate and along the lines created by the EUV-IL process. More recently, Shin et al. created perpendicular lamellae of PS-*b*-PMMA on top of a broad stripe (several L_0 wide) of neutral surface in a field of preferential surface; the lamellar normal faithfully tracked the centerline of the neutral stripe even when the stripe bent (129).

Advanced lithographic techniques, such as EUV-IL and e-beam lithography, can create features on the same scale as the block copolymer microdomains. By using such patterning techniques, one can move from graphoepitaxy—which is limited in the translational order it can provide—to true epitaxy at the microdomain length scale, in which both orientational and translational order of the microdomains persist over the entire pattern. Nealey and coworkers first demonstrated this approach by using EUV-IL to pattern alternating lines and spaces into a photoresist and then using this mask to alter the chemistry of the underlying phenylethyltrichlorosilane (PETS) (59, 130) or to selectively remove the underlying PS-*r*-PMMA brush layer (131) to induce lamellae-forming PS-*b*-PMMA to follow the interference pattern. They tested the impact of incommensurability between L_0 and L_S (the period of the chemical pattern—easily tunable using EUV-IL) on the degree of order and types of defects present. Perfect, defect-free registration was observed when $L_S = L_0$, but they also observed dislocation dipoles when $L_S < L_0$, lamellae tilted away from the surface normal when $L_S > L_0$, and unregistered lamellae when L_S and L_0 differed by more than 10%. Edwards et al. investigated the effect that the relative width of the two types of stripes that form the pattern has on the quality of order and the angle that the lamellar interface makes with the surface; they found the best pattern registry and broadest tolerance for relative stripe width variations when $L_S \approx L_0$ (132). The mechanism

and kinetics of the ordering of block copolymer films on such epitaxially patterned substrates were also investigated; initially, hexagonally-packed PS domains form, which coalesce to create defect-heavy linear domains not fully registered with the chemical pattern (133). The defects coarsen by breaking the PS domains until registered lamellae form. Edwards et al. were also able to orient cylinder-forming PS-*b*-PMMA block copolymer thin films with the cylinder axes following the stripe-patterned substrate (134), and later Park et al. demonstrated the ability to create a defect-free hexagonal array of dots using sphere-forming PS-*b*-PMMA on a striped pattern (135). For the sphere- and cylinder-forming block copolymers, the film thickness is critically important; ordered structures are observed only when the thickness is commensurate with L_0 because hemicylinders wet the preferential surface stripes and induce alignment of the sphere or cylinder caps above. Complex structures are also possible, such as alternating parallel and perpendicular arrays of cylinder-forming PS-*b*-PMMA, which may be created using a combination of incommensurate surface patterns ($L_S = 100$ nm and $L_0 = 45$ nm) and very thin films ($d = 20$ nm) (136). Dense arrays of hexagonal cylinders oriented perpendicular to the surface can be formed by chemically patterning dots commensurate with the cylinder spacing of PS-*b*-PMMA (137).

The examples reviewed in the preceding paragraph all employ a 1:1 relationship between the surface pattern and the block copolymer microdomain lattice, thereby limiting the feature density to that written into the pattern. But recently, work has been done to "frequency multiply" the block copolymer chemical pattern by using a block copolymer whose period is a submultiple of the chemical pattern. Ruiz et al. and Tada et al. were able to obtain a fourfold increase in dot number density using hexagonal dot patterns with $L_S = 2L_0$ for cylinder-forming PS-*b*-PMMA with no loss in orientational control or increase in defects (138, 139). The dots had an affinity for the PMMA cylinders, whereas the rest of the substrate was slightly preferential for the PS block. Later, Tada et al. were able to extend this to a ninefold increase with similar results (140). Xiao et al. used e-beam lithography to create dots on the substrate preferential for the minority PDMS component in a sphere-forming PS-*b*-PDMS diblock, demonstrating frequency multiplication by a factor of nine with translational order extending over the entire patterned area (141). Bita et al. used e-beam lithography to template a sparse array of posts that have a preferential affinity for one block in a sphere-forming PS-*b*-PDMS, which yielded exceptional control of positional order (**Figure 7**) (142). The posts replace one of the domains, and then self-assembly of the block copolymer fills in the remainder of the lattice. The authors placed the posts at points commensurate with the block copolymer lattice (i.e., $\langle 3\ 0 \rangle$, indicating that a post is placed along one of the basis vectors but at three times the spacing) and found that control is still maintained up to $L_{post}/L_0 = 5$, although degenerate states are observed (self-assembly on a $\langle 2\ 1 \rangle$ configuration led to grains of $\pm$ 19° randomly separated by grain boundaries). To eliminate this degeneracy, posts were added that corresponded to the orientation sought. Bita et al. also found that different sizes and shapes of the posts still induce the desired orientation and control as long as the spacing of the posts is commensurate with the microdomain spacing.

The examples of microdomain epitaxy reviewed in the paragraph above employ substrates patterned with regular arrays of stripes or dots, but the flexible nature of e-beam lithography allows features of essentially arbitrary shape and placement to be created on the substrate, including irregular or isolated features. Stoykovich et al. used e-beam lithography to create a chemically patterned substrate having an array of bends with angles from 45° to 135° (143). Lamellae-forming PS-*b*-PMMA/PS/PMMA ternary blends were then placed on this patterned substrate and, if L_S was commensurate with L_0, the blend microdomains followed the pattern perfectly. Homopolymer addition was necessary to mitigate the free energy cost of locally stretching the lamellae at the

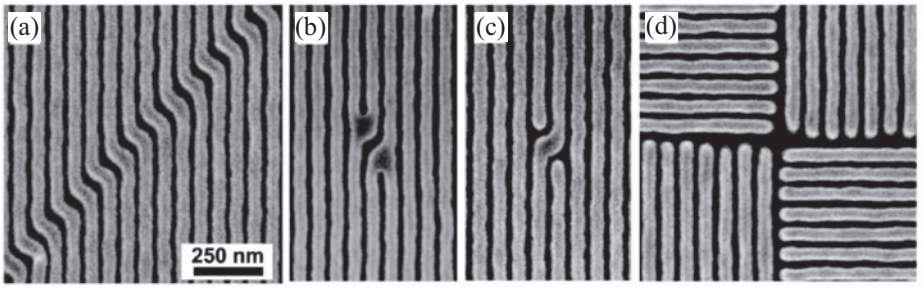

Figure 8

Scanning electron micrographs of PS-*b*-PMMA/PS/PMMA ternary blends placed on chemical patterns to showcase the complex features possible using block copolymers: (*a*) dense array of jogs, (*b*) isolated PMMA jog, (*c*) isolated PS jog, and (*d*) arrays of T-junctions. Reproduced with permission from Reference 145. Copyright © 2007, American Chemical Society.

bend. Other interesting and complex patterns were possible with this technique. Kang et al. were able to create block copolymer assemblies on arrays of rectangles, alternating lines and dashes, or on checkerboard trimming patterns by adjusting L_S, L_0, overall fraction of the PS block (φ_S), total homopolymer fraction (φ_H), and fraction of the chemical pattern preferentially wetted by PS (F_S) in a PS-*b*-PMMA/PS/PMMA ternary blend (144). Essential structures for integrated circuit geometries, such as dense arrays of jogs and T-junctions and isolated segments (**Figure 8**), were obtained in PS-*b*-PMMA/PS/PMMA blends by using e-beam lithography to chemically pattern the substrate (145). Wilmes et al. bent a lamellae-forming PS-*b*-PMMA into concentric circles using a chemically-patterned substrate (146). Finally, Cheng et al. combined several of the attributes of block copolymer films noted above—the ability to follow a curved substrate pattern, tolerance for defects in this pattern, and the ability to frequency-multiply—to create a dense concentric-circle pattern (**Figure 9**) from lamellae-forming PS-*b*-PMMA; the chemical pattern is twice L_0 (147). The "bullseye" pattern is free from defects over its entire 4-μm diameter despite substantial local variations in line widths and numerous line breaks in the underlying pattern.

CONCLUSIONS AND OUTLOOK

Manipulating structures on the tens of nanometers scale is not a trivial problem to tackle. Luckily, block copolymers can microphase-separate into dense, well-defined spherical, cylindrical, or lamellar structures over large areas without assistance, but the direct use of such patterns for nanolithographic applications is limited owing to uncontrolled nucleation and growth of the microdomains as small grains. Many techniques have been developed to guide the self-assembly process, with varying degrees of success. The desired application and its tolerance to the quality of order will dictate which technique will be best suited. Solvent annealing and thermal treatments (either annealing or passing the block copolymer through a solidification front) can generate large, defect-free areas, but without control over the in-plane orientation of the microdomains. In-plane orientation can be obtained by using a sweeping temperature gradient, a thickness gradient, or directional crystallization of a solvent, or by applying an external field such as flow or an electric field, all of which are relatively rapid and facile processes. However, residual dislocations remain that limit the translational order possible with these techniques. Pretreating a surface to create

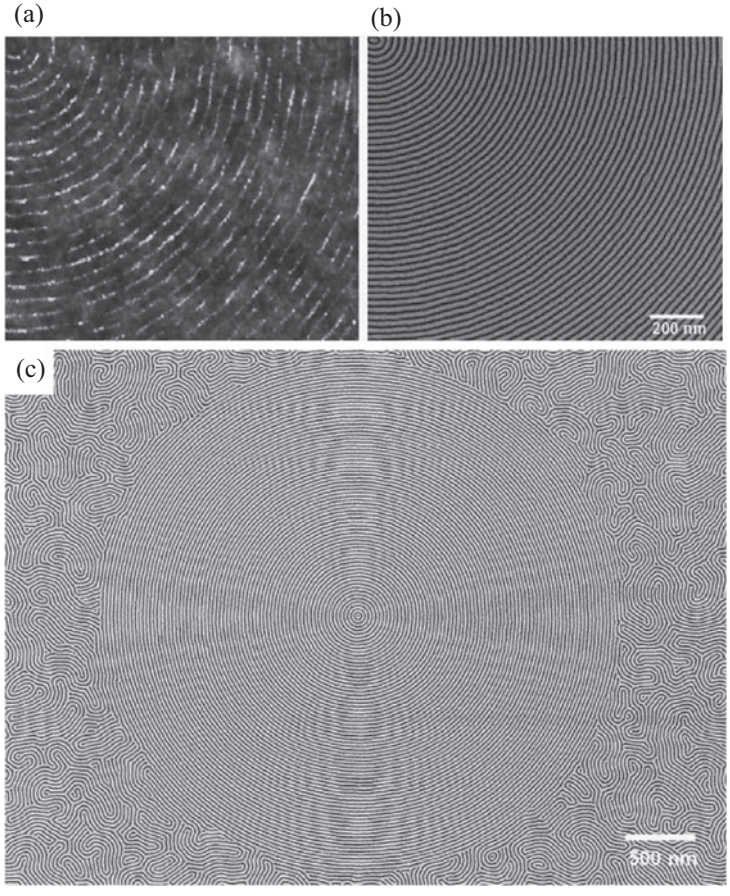

Figure 9

Example of frequency doubling and defect tolerance on curved stripe patterns. (*a*) Atomic force micrograph of a chemical pattern with spacing of $L_S = 2L_0$ for lamellae-forming PS-*b*-PMMA block copolymers, which displays many defects. (*b*) and (*c*) Scanning electron micrographs showing that the PS-*b*-PMMA perfectly follows the chemical pattern, doubling the pattern frequency and disregarding the many breaks in the pattern. Reproduced with permission from Reference 147. Copyright © 2008, Wiley-VCH Verlag GmbH & Co. KGaA.

either topographic structures or chemical patterns is currently the only way to control the orientational and positional order completely, although the areal coverage using these techniques is presently limited. In conjunction with many of these techniques, the out-of-plane orientation of the microdomains can be controlled by altering the surface (either by neutralizing or roughening it), by including additives in the block copolymer (nanoparticles, homopolymers), by using out-of-plane electric fields, or by employing solvent vapor treatments. Work will continue on many of these techniques to reduce residual defects, to enhance the speed of the alignment process, and/or to increase the area of the oriented structures. Also, the use of more complex materials, such as liquid crystal block copolymers, ABC block copolymers, or functional block copolymers, which have not been investigated in much detail, could lead to very interesting alignment and phase behavior useful for nanopatterning.

SUMMARY POINTS

1. As-cast block copolymer thin films lack the orientational and/or positional control necessary for utilization as nanolithographic etch masks for many desired applications.
2. Altering the out-of-plane orientation of the microdomains requires techniques that overcome the effect that differing surface energies have on the film. One can change the substrate (neutralize with copolymer brushes, roughen the substrate, or chemically pattern the substrate), include additives in the block copolymer (nanoparticles, homopolymers), or use external forces (electric fields, solvent evaporation).
3. Large, defect-free grains can be formed by thermal treatment or solvent annealing.
4. Lateral orientational control of the microdomains can be created using temperature gradients, thickness gradients, corrugated substrates, electric fields, shearing fields, or epitaxial crystallization, although these techniques yield films that contain residual dislocations that limit control over the positional order.
5. Lateral positional control of the microdomains can be achieved with topographic features (either a step edge or individual posts of comparable size with microdomain size) or chemically patterned substrates, although patterning techniques such as electron-beam lithography limit the areal coverage possible.

FUTURE ISSUES

1. Can techniques be combined so that large-area, defect-free thin films can be created?
2. Will block copolymers with differing architectures respond similarly to the alignment processes successful for the linear di/triblock copolymers reviewed here?
3. Do other self-assembling materials exist that are susceptible to other alignment processes and can be combined with block copolymers?

DISCLOSURE STATEMENT

The authors are not aware of any affiliations, memberships, funding, or financial holdings that might be perceived as affecting the objectivity of this review.

ACKNOWLEDGMENTS

We would like to apologize to any researcher whose work we were unable to include in this review owing to space constraints. We gratefully acknowledge financial support from the National Science Foundation MRSEC Program through the Princeton Center for Complex Materials (DMR-0819860) and from the Princeton University Graduate School through a Harold W. Dodds Honorific Fellowship to A.P.M. We also acknowledge our many collaborators in this area over the past 15 years, most especially our continuing collaboration with Paul Chaikin (New York University).

LITERATURE CITED

1. Bates FS. 1991. Polymer-polymer phase behavior. *Science* 251:898–905
2. Hamley IW. 1998. *The Physics of Block Copolymers*. Oxford: Oxford Univ. Press
3. Park M, Harrison C, Chaikin PM, Register RA, Adamson DH. 1997. Block copolymer lithography: periodic arrays of $\sim 10^{11}$ holes in 1 square centimeter. *Science* 276:1401–4
4. Segalman RA. 2005. Patterning with block copolymer thin films. *Mater. Sci. Eng. Rep.* 48:191–226
5. Harrison C, Dagata JA, Adamson DH. 2004. Lithography with self-assembled block copolymer microdomains. In *Developments in Block Copolymer Science and Technology*, ed. IW Hamley, pp. 295–323. Chichester: Wiley
6. Trawick ML, Angelescu DE, Chaikin PM, Register RA. 2005. Block copolymer nanolithography. In *Non-Conventional Lithography and Patterning: Techniques and Applications*, ed. DG Bucknall, pp. 1–38. Cambridge, UK: Woodhead
7. Park C, Yoon J, Thomas EL. 2003. Enabling nanotechnology with self assembled block copolymer patterns. *Polymer* 44:6725–60
8. Hamley IW. 2003. Nanostructure fabrication using block copolymers. *Nanotechnology* 14:R39–54
9. Pelletier V, Asakawa K, Wu M, Adamson DH, Register RA, Chaikin PM. 2006. Aluminum nanowire polarizing grids: fabrication and analysis. *Appl. Phys. Lett.* 88:211114
10. Hong Y-R, Asakawa K, Adamson DH, Chaikin PM, Register RA. 2007. Silicon nanowire grid polarizer for very deep UV fabricated from a shear-aligned diblock copolymer template. *Opt. Lett.* 32:3125–27
11. Thurn-Albrecht T, Schotter J, Kastle GA, Emley N, Shibauchi T, et al. 2000. Ultrahigh-density nanowire arrays grown in self-assembled diblock copolymer templates. *Science* 290:2126–29
12. Park M, Chaikin PM, Register RA, Adamson DH. 2001. Large area dense nanoscale patterning of arbitrary surfaces. *Appl. Phys. Lett.* 79:257–59
13. Shin K, Leach KA, Goldbach JT, Kim DH, Jho JY, et al. 2002. A simple route to metal nanodots and nanoporous metal films. *Nano Lett.* 2:933–36
14. Naito K, Hieda H, Sakurai M, Kamata Y, Asakawa K. 2002. 2.5-inch disk patterned media prepared by an artificially assisted self-assembling method. *IEEE Trans. Mag.* 38:1949–51
15. Hillmyer M. 2005. Nanoporous materials from block copolymer precursors. *Adv. Polym. Sci.* 190:137–81
16. Olson DA, Chen L, Hillmyer MA. 2007. Templating nanoporous polymers with ordered block copolymers. *Chem. Mater.* 20:869–90
17. Kim BJ, Fredrickson GH, Kramer EJ. 2007. Effect of polymer ligand molecular weight on polymer-coated nanoparticle location in block copolymers. *Macromolecules* 41:436–47
18. Liu G, Zhao J. 2006. Guided alignment and positioning of single DNA molecules by a structured contact line on a block copolymer surface. *Langmuir* 22:2923–26
19. Anastasiadis SH, Retsos H, Pispas S, Hadjichristidis N, Neophytides S. 2003. Smart polymer surfaces. *Macromolecules* 36:1994–99
20. Bates FS, Fredrickson GH. 2003. Block copolymer thermodynamics: theory and experiment. *Annu. Rev. Phys. Chem.* 41:525–57
21. Matsen MW, Bates FS. 1996. Unifying weak- and strong-segregation block copolymer theories. *Macromolecules* 29:1091–98
22. Bates FS, Fredrickson GH. 1999. Block copolymers–designer soft materials. *Phys. Today* 52(2):32–38
23. Lynd NA, Meuler AJ, Hillmyer MA. 2008. Polydispersity and block copolymer self-assembly. *Prog. Polym. Sci.* 33:875–93
24. Zheng W, Wang Z-G. 2002. Morphology of ABC triblock copolymers. *Macromolecules* 28:7215–23
25. Jiang Z, Wang R, Xue G. 2009. Morphology and phase diagram of comb block copolymer $A_{m+1}(BC)_m$. *J. Phys. Chem. B* 113:7462–67
26. Lee WB, Elliott R, Mezzenga R, Fredrickson GH. 2009. Novel phase morphologies in a microphase-separated dendritic polymer melt. *Macromolecules* 42:849–59
27. Russell TP, Coulon G, Deline VR, Miller DC. 1989. Characteristics of the surface-induced orientation for symmetric diblock PS/PMMA copolymers. *Macromolecules* 22:4600–6
28. Coulon G, Russell TP, Deline VR, Green PF. 1989. Surface-induced orientation of symmetric, diblock copolymers: a secondary ion mass-spectrometry study. *Macromolecules* 22:2581–89

29. Coulon G, Ausserre D, Russell TP. 1990. Interference microscopy on thin diblock copolymer films. *J. Phys. France* 51:777–86
30. Coulon G, Collin B, Ausserre D, Chatenay D, Russell TP. 1990. Islands and holes on the free surface of thin diblock copolymer films. I. Characteristics of formation and growth. *J. Phys. Fr.* 51:2801–11
31. Fasolka MJ, Banerjee P, Mayes AM, Pickett G, Balazs AC. 2000. Morphology of ultrathin supported diblock copolymer films: theory and experiment. *Macromolecules* 33:5702–12
32. Harrison C, Chaikin PM, Huse DA, Register RA, Adamson DH, et al. 1999. Reducing substrate pinning of block copolymer microdomains with a buffer layer of polymer brushes. *Macromolecules* 33:857–65
33. Harrison C, Park M, Chaikin P, Register RA, Adamson DH, Yao N. 1998. Depth profiling block copolymer microdomains. *Macromolecules* 31:2185–89
34. Zhang X, Berry BC, Yager KG, Kim S, Jones RL, et al. 2008. Surface morphology diagram for cylinder-forming block copolymer thin films. *ACS Nano* 2:2331–41
35. Horvat A, Knoll A, Krausch G, Tsarkova L, Lyakhova KS, et al. 2007. Time evolution of surface relief structures in thin block copolymer films. *Macromolecules* 40:6930–39
36. Knoll A, Horvat A, Lyakhova KS, Krausch G, Sevink GJA, et al. 2002. Phase behavior in thin films of cylinder-forming block copolymers. *Phys. Rev. Lett.* 89:035501
37. Horvat A, Lyakhova KS, Sevink GJA, Zvelindovsky AV, Magerle R. 2004. Phase behavior in thin films of cylinder-forming ABA block copolymers: mesoscale modeling. *J. Chem. Phys.* 120:1117–26
38. Niihara K-I, Sugimori H, Matsuwaki U, Hirato F, Morita H, et al. 2008. A transition from cylindrical to spherical morphology in diblock copolymer thin films. *Macromolecules* 41:9318–25
39. Yokoyama H, Mates TE, Kramer EJ. 2000. Structure of asymmetric diblock copolymers in thin films. *Macromolecules* 33:1888–98
40. Stein GE, Cochran EW, Katsov K, Fredrickson GH, Kramer EJ, et al. 2007. Symmetry breaking of in-plane order in confined copolymer mesophases. *Phys. Rev. Lett.* 98:158302
41. Stein GE, Kramer EJ, Li X, Wang J. 2007. Layering transitions in thin films of spherical-domain block copolymers. *Macromolecules* 40:2453–60
42. Mayes AM, Russell TP, Satija SK, Majkrzak CF. 1992. Homopolymer distributions in ordered block copolymers. *Macromolecules* 25:6523–31
43. Jeong U, Ryu DY, Kho DH, Lee DH, Kim JK, Russell TP. 2003. Phase behavior of mixtures of block copolymer and homopolymers in thin films and bulk. *Macromolecules* 36:3626–34
44. Liu G, Stoykovich MP, Ji S, Stuen KO, Craig GSW, Nealey PF. 2009. Phase behavior and dimensional scaling of symmetric block copolymers-homopolymer ternary blends in thin films. *Macromolecules* 42:3063–72
45. Stuen KO, Thomas CS, Liu G, Ferrier N, Nealey PF. 2009. Dimensional scaling of cylinders in thin films of block copolymer-homopolymer ternary blends. *Macromolecules* 42:5139–45
46. Pickett GT, Witten TA, Nagel SR. 2002. Equilibrium surface orientation of lamellae. *Macromolecules* 26:3194–99
47. Peters RD, Yang XM, Kim TK, Sohn BH, Nealey PF. 2000. Using self-assembled monolayers exposed to X-rays to control the wetting behavior of thin films of diblock copolymers. *Langmuir* 16:4625–31
48. Mansky P, Russell TP, Hawker CJ, Mays J, Cook DC, Satija SK. 1997. Interfacial segregation in disordered block copolymers: effect of tunable surface potentials. *Phys. Rev. Lett.* 79:237–40
49. Mansky P, Russell TP, Hawker CJ, Pitsikalis M, Mays J. 1997. Ordered diblock copolymer films on random copolymer brushes. *Macromolecules* 30:6810–13
50. Ham S, Shin C, Kim E, Ryu DY, Jeong U, et al. 2008. Microdomain orientation of PS-*b*-PMMA by controlled interfacial interactions. *Macromolecules* 41:6431–37
51. Han E, Stuen KO, La Y-H, Nealey PF, Gopalan P. 2008. Effect of composition of substrate-modifying random copolymers on the orientation of symmetric and asymmetric diblock copolymer domains. *Macromolecules* 41:9090–97
52. Ji S, Liu G, Zheng F, Craig GSW, Himpsel FJ, Nealey PF. 2008. Preparation of neutral wetting brushes for block copolymer films from homopolymer blends. *Adv. Mater.* 20:3054–60
53. Ji S, Liu C-C, Son JG, Gotrik K, Craig GSW, et al. 2008. Generalization of the use of random copolymers to control the wetting behavior of block copolymer films. *Macromolecules* 41:9098–103

54. Huang E, Mansky P, Russell TP, Harrison C, Chaikin PM, et al. 1999. Mixed lamellar films: evolution, commensurability effects, and preferential defect formation. *Macromolecules* 33:80–88
55. Tsori Y, Andelman D. 2003. Parallel and perpendicular lamellae on corrugated surfaces. *Macromolecules* 36:8560–66
56. Sivaniah E, Hayashi Y, Iino M, Hashimoto T, Fukunaga K. 2003. Observation of perpendicular orientation in symmetric diblock copolymer thin films on rough substrates. *Macromolecules* 36:5894–96
57. Maire HC, Ibrahim S, Li Y, Ito T. 2009. Effects of substrate roughness on the orientation of cylindrical domains in thin films of a polystyrene-poly(methylmethacrylate) diblock copolymer studied using atomic force microscopy and cyclic voltammetry. *Polymer* 50:2273–80
58. Yager KG, Berry BC, Page K, Patton D, Karim A, Amis EJ. 2009. Disordered nanoparticle interfaces for directed self-assembly. *Soft Matter* 5:622–28
59. Kim SO, Solak HH, Stoykovich MP, Ferrier NJ, de Pablo JJ, Nealey PF. 2003. Epitaxial self-assembly of block copolymers on lithographically defined nanopatterned substrates. *Nature* 424:411–14
60. Lin Y, Boker A, He J, Sill K, Xiang H, et al. 2005. Self-directed self-assembly of nanoparticle/copolymer mixtures. *Nature* 434:55–59
61. Park SC, Kim BJ, Hawker CJ, Kramer EJ, Bang J, Ha JS. 2007. Controlled ordering of block copolymer thin films by the addition of hydrophilic nanoparticles. *Macromolecules* 40:8119–24
62. Jeong U, Ryu DY, Kho DH, Kim JK, Goldbach JT, et al. 2004. Enhancement in the orientation of the microdomain in block copolymer thin films upon the addition of homopolymer. *Adv. Mater.* 16:533–36
63. Wang J-Y, Chen W, Sievert JD, Russell TP. 2008. Lamellae orientation in block copolymer films with ionic complexes. *Langmuir* 24:3545–50
64. Khanna V, Cochran EW, Hexemer A, Stein GE, Fredrickson GH, et al. 2006. Effect of chain architecture and surface energies on the ordering behavior of lamellar and cylinder forming block copolymers. *Macromolecules* 39:9346–56
65. Kubo T, Wang RF, Olson DA, Rodwogin M, Hillmyer MA, Leighton C. 2008. Spontaneous alignment of self-assembled ABC triblock terpolymers for large-area nanolithography. *Appl. Phys. Lett.* 93:133112
66. Thurn-Albrecht T, DeRouchey J, Russell TP, Jaeger HM. 2000. Overcoming interfacial interactions with electric fields. *Macromolecules* 33:3250–53
67. Thurn-Albrecht T, DeRouchey J, Russell TP, Kolb R. 2002. Pathways toward electric field induced alignment of block copolymers. *Macromolecules* 35:8106–10
68. Xu T, Zvelindovsky AV, Sevink GJA, Lyakhova KS, Jinnai H, Russell TP. 2005. Electric field alignment of asymmetric diblock copolymer thin films. *Macromolecules* 38:10788–98
69. Xu T, Zhu Y, Gido SP, Russell TP. 2004. Electric field alignment of symmetric diblock copolymer thin films. *Macromolecules* 37:2625–29
70. Voicu NE, Ludwigs S, Steiner U. 2008. Alignment of lamellar block copolymers via electrohydrodynamic-driven micropatterning. *Adv. Mater.* 20:3022–27
71. Park S, Kim B, Xu J, Hofmann T, Ocko BM, Russell TP. 2009. Lateral ordering of cylindrical microdomains under solvent vapor. *Macromolecules* 42:1278–84
72. Harrison C, Cheng Z, Sethuraman S, Huse DA, Chaikin PM, et al. 2002. Dynamics of pattern coarsening in a two-dimensional smectic system. *Phys. Rev. E* 66:011706
73. Harrison C, Adamson DH, Cheng Z, Sebastian JM, Sethuraman S, et al. 2000. Mechanisms of ordering in striped patterns. *Science* 290:1558–60
74. Harrison C, Angelescu DE, Trawick M, Cheng Z, Huse DA, et al. 2004. Pattern coarsening in a 2D hexagonal system. *Europhys. Lett.* 67:800–6
75. Horvat A, Sevink GJA, Zvelindovsky AV, Krekhov A, Tsarkova L. 2008. Specific features of defect structure and dynamics in the cylinder phase of block copolymers. *ACS Nano* 2:1143–52
76. Angelescu DE, Waller JH, Adamson DH, Register RA, Chaikin PM. 2007. Enhanced order of block copolymer cylinders in single-layer films using a sweeping solidification front. *Adv. Mater.* 19:2687–90
77. Kim G, Libera M. 1998. Morphological development in solvent-cast polystyrene-polybutadiene-polystyrene (SBS) triblock copolymer thin films. *Macromolecules* 31:2569–77
78. Lin ZQ, Kim DH, Wu XD, Boosahda L, Stone D, et al. 2002. A rapid route to arrays of nanostructures in thin films. *Adv. Mater.* 14:1373–76

79. Kim SH, Misner MJ, Xu T, Kimura M, Russell TP. 2004. Highly oriented and ordered arrays from block copolymers via solvent evaporation. *Adv. Mater.* 16:226–31
80. Chen Y, Huang H, Hu Z, He T. 2004. Lateral nanopatterns in thin diblock copolymer films induced by selective solvents. *Langmuir* 20:3805–8
81. Berry BC, Bosse AW, Douglas JF, Jones RL, Karim A. 2007. Orientational order in block copolymer films zone annealed below the order-disorder transition temperature. *Nano Lett.* 7:2789–94
82. Bosse AW, Douglas JF, Berry BC, Jones RL, Karim A. 2007. Block-copolymer ordering with a spatiotemporally heterogeneous mobility. *Phys. Rev. Lett.* 99:216101
83. Kim BH, Shin DO, Jeong S-J, Koo CM, Jeon SC, et al. 2008. Hierarchical self-assembly of block copolymers for lithography-free nanopatterning. *Adv. Mater.* 20:2303–7
84. Kim BH, Lee HM, Lee J-H, Son S-W, Jeong S-J, et al. 2009. Spontaneous lamellar alignment in thickness-modulated block copolymer films. *Adv. Funct. Mater.* 19:2584–91
85. Kim H-C, Rettner CT, Sundstrom L. 2008. Fabrication of 20 nm half-pitch gratings by corrugation-directed self-assembly. *Nanotechnology* 19:235301
86. Park S-M, Berry BC, Dobisz E, Kim H-C. 2009. Observation of surface corrugation-induced alignment of lamellar microdomains in PS-*b*-PMMA thin films. *Soft Matter* 5:957–61
87. Park S, Lee DH, Xu J, Kim B, Hong SW, et al. 2009. Macroscopic 10-terabit-per-square-inch arrays from block copolymers with lateral order. *Science* 323:1030–33
88. Morkved TL, Lu M, Urbas AM, Ehrichs EE, Jaeger HM, et al. 1996. Local control of microdomain orientation in diblock copolymer thin films with electric fields. *Science* 273:931–33
89. Mansky P, DeRouchey J, Russell TP, Mays J, Pitsikalis M, et al. 1998. Large-area domain alignment in block copolymer thin films using electric fields. *Macromolecules* 31:4399–401
90. Albalak RJ, Thomas EL. 1993. Microphase separation of block copolymer solutions in a flow field. *J. Polym. Sci. Part B* 31:37–46
91. Kimura M, Misner MJ, Xu T, Kim SH, Russell TP. 2003. Long-range ordering of diblock copolymers induced by droplet pinning. *Langmuir* 19:9910–13
92. Angelescu DE, Waller JH, Adamson DH, Deshpande P, Chou SY, et al. 2004. Macroscopic orientation of block copolymer cylinders in single-layer films by shearing. *Adv. Mater.* 16:1736–40
93. Angelescu DE, Waller JH, Register RA, Chaikin PM. 2005. Shear-induced alignment in thin films of spherical nanodomains. *Adv. Mater.* 17:1878–81
94. Wu MW, Register RA, Chaikin PM. 2006. Shear alignment of sphere-morphology block copolymer thin films with viscous fluid flow. *Phys. Rev. E* 74:040801
95. Pelletier V, Adamson DH, Register RA, Chaikin PM. 2007. Writing mesoscale patterns in block copolymer thin films through channel flow of a nonsolvent fluid. *Appl. Phys. Lett.* 90:163105
96. Marencic AP, Wu MW, Register RA, Chaikin PM. 2007. Orientational order in sphere-forming block copolymer thin films aligned under shear. *Macromolecules* 40:7299–305
97. Marencic AP, Adamson DH, Chaikin PM, Register RA. 2010. Shear-alignment and realignment of sphere-forming and cylinder-forming block copolymer thin films. *Phys. Rev. E* 81:011503
98. Arya G, Panagiotopoulos AZ. 2004. Monte Carlo study of shear-induced alignment of cylindrical micelles in thin films. *Phys. Rev. E* 70:031501
99. Arya G, Rottler J, Panagiotopoulos AZ, Srolovitz DJ, Chaikin PM. 2005. Shear ordering in thin films of spherical block copolymer. *Langmuir* 21:11518–27
100. Hong Y-R, Adamson DH, Chaikin PM, Register RA. 2009. Shear-induced sphere-to-cylinder transition in diblock copolymer thin films. *Soft Matter* 5:1687–91
101. Yu H, Iyoda T, Ikeda T. 2006. Photoinduced alignment of nanocylinders by supramolecular cooperative motions. *J. Am. Chem. Soc.* 128:11010–11
102. Morikawa Y, Nagano S, Watanabe K, Kamata K, Iyoda T, Seki T. 2006. Optical alignment and patterning of nanoscale microdomains in a block copolymer thin film. *Adv. Mater.* 18:883–86
103. Morikawa Y, Kondo T, Nagano S, Seki T. 2007. Photoinduced 3D ordering and patterning of microphase-separated nanostructure in polystyrene-based block copolymer. *Chem. Mater.* 19:1540–42
104. De Rosa C, Park C, Lotz B, Wittmann J-C, Fetters LJ, Thomas EL. 2000. Control of molecular and microdomain orientation in a semicrystalline block copolymer thin film by epitaxy. *Macromolecules* 33:4871–76

105. De Rosa C, Park C, Thomas EL, Lotz B. 2000. Microdomain patterns from directional eutectic solidification and epitaxy. *Nature* 405:433–37
106. Park C, De Rosa C, Thomas EL. 2001. Large area orientation of block copolymer microdomains in thin films via directional crystallization of a solvent. *Macromolecules* 34:2602–6
107. Park C, Cheng JY, Fasolka MJ, Mayes AM, Ross CA, et al. 2001. Double textured cylindrical block copolymer domains via directional solidification on a topographically patterned substrate. *Appl. Phys. Lett.* 79:848–50
108. Segalman RA, Yokoyama H, Kramer EJ. 2001. Graphoepitaxy of spherical domain block copolymer films. *Adv. Mater.* 13:1152–55
109. Segalman RA, Hexemer A, Kramer EJ. 2003. Effects of lateral confinement on order in spherical domain block copolymer thin films. *Macromolecules* 36:6831–39
110. Cheng JY, Ross CA, Thomas EL, Smith HI, Vancso GJ. 2002. Fabrication of nanostructures with long-range order using block copolymer lithography. *Appl. Phys. Lett.* 81:3657–59
111. Cheng JY, Ross CA, Thomas EL, Smith HI, Vancso GJ. 2003. Templated self-assembly of block copolymers: effect of substrate topography. *Adv. Mater.* 15:1599–602
112. Cheng JY, Mayes AM, Ross CA. 2004. Nanostructure engineering by templated self-assembly of block copolymers. *Nat. Mater.* 3:823–28
113. Cheng JY, Zhang F, Chuang VP, Mayes AM, Ross CA. 2006. Self-assembled one-dimensional nanostructure arrays. *Nano Lett.* 6:2099–103
114. Cheng JY, Zhang F, Smith HI, Vancso GJ, Ross CA. 2006. Pattern registration between spherical block-copolymer domains and topographical templates. *Adv. Mater.* 18:597–601
115. Hexemer A, Stein GE, Kramer EJ, Magonov S. 2005. Block copolymer monolayer structure measured with scanning force microscopy moire patterns. *Macromolecules* 38:7083–89
116. Stein GE, Kramer EJ, Li X, Wang J. 2007. Single-crystal diffraction from two-dimensional block copolymer arrays. *Phys. Rev. Lett.* 98:086101
117. Stein GE, Lee WB, Fredrickson GH, Kramer EJ, Li X, Wang J. 2007. Thickness dependent ordering in laterally confined monolayers of spherical-domain block copolymers. *Macromolecules* 40:5791–800
118. Bosse AW, Garcia-Cervera CJ, Fredrickson GH. 2007. Microdomain ordering in laterally confined block copolymer thin films. *Macromolecules* 40:9570–81
119. Hur S-M, Garcia-Cervera CJ, Kramer EJ, Fredrickson GH. 2009. SCFT simulations of thin film blends of block copolymer and homopolymer laterally confined in a square well. *Macromolecules* 42:5861–72
120. Sundrani D, Darling SB, Sibener SJ. 2003. Guiding polymers to perfection: macroscopic alignment of nanoscale domains. *Nano Lett.* 4:273–76
121. Sundrani D, Darling SB, Sibener SJ. 2004. Hierarchical assembly and compliance of aligned nanoscale polymer cylinders in confinement. *Langmuir* 20:5091–99
122. Park S-M, Stoykovich MP, Ruiz R, Zhang Y, Black CT, Nealey PF. 2007. Directed assembly of lamellae-forming block copolymers by using chemically and topographically patterned substrates. *Adv. Mater.* 19:607–11
123. Sundrani D, Sibener SJ. 2002. Spontaneous spatial alignment of polymer cylindrical nanodomains on silicon nitride gratings. *Macromolecules* 35:8531–39
124. Park S-M, Rettner CT, Pitera JW, Kim H-C. 2009. Directed self-assembly of lamellar microdomains of block copolymers using topographic guiding patterns. *Macromolecules* 42:5895–99
125. Yamaguchi T, Yamaguchi H. 2008. Two-dimensional patterning of flexible designs with high half-pitch resolution by using block copolymer lithography. *Adv. Mater.* 20:1684–89
126. Jeong S-J, Kim JE, Moon H-S, Kim BH, Kim SM, et al. 2009. Soft graphoepitaxy of block copolymer assembly with disposable photoresist confinement. *Nano Lett.* 9:2300–5
127. Park S-M, Park O-H, Cheng JY, Rettner CT, Kim H-C. 2008. Patterning sub-10 nm line patterns from a block copolymer hybrid. *Nanotechnology* 19:455304
128. Yang XM, Peters RD, Nealey PF, Solak HH, Cerrina F. 2000. Guided self-assembly of symmetric diblock copolymer films on chemically nanopatterned substrates. *Macromolecules* 33:9575–82
129. Shin DO, Kim BH, Kang J-H, Jeong S-J, Park SH, et al. 2009. One-dimensional nanoassembly of block copolymers tailored by chemically patterned surfaces. *Macromolecules* 42:1189–93

130. Kim SO, Kim BH, Kim K, Koo CM, Stoykovich MP, et al. 2006. Defect structure in thin films of a lamellar block copolymer self-assembled on neutral homogeneous and chemically nanopatterned surfaces. *Macromolecules* 39:5466–70
131. Edwards EW, Montague MF, Solak HH, Hawker CJ, Nealey PF. 2004. Precise control over molecular dimensions of block-copolymer domains using the interfacial energy of chemically nanopatterned substrates. *Adv. Mater.* 16:1315–19
132. Edwards EW, Muller M, Stoykovich MP, Solak HH, de Pablo JJ, Nealey PF. 2007. Dimensions and shapes of block copolymer domains assembled on lithographically defined chemically patterned substrates. *Macromolecules* 40:90–96
133. Edwards EW, Stoykovich MP, Müller M, Solak HH, de Pablo JJ, Nealey PF. 2005. Mechanism and kinetics of ordering in diblock copolymer thin films on chemically nanopatterned substrates. *J. Polym. Sci. Part B* 43:3444–59
134. Edwards EW, Stoykovich MP, Solak HH, Nealey PF. 2006. Long-range order and orientation of cylinder-forming block copolymers on chemically nanopatterned striped surfaces. *Macromolecules* 39:3598–607
135. Park S-M, Craig GSW, La Y-H, Nealey PF. 2008. Morphological reconstruction and ordering in films of sphere-forming block copolymers on striped chemically patterned surfaces. *Macromolecules* 41:9124–29
136. Kim SO, Kim BH, Meng D, Shin DO, Koo CM, et al. 2007. Novel complex nanostructure from directed assembly of block copolymers on incommensurate surface patterns. *Adv. Mater.* 19:3271–75
137. Park S-M, Craig GSW, Liu C-C, La Y-H, Ferrier NJ, Nealey PF. 2008. Characterization of cylinder-forming block copolymers directed to assemble on spotted chemical patterns. *Macromolecules* 41:9118–23
138. Ruiz R, Kang H, Detcheverry FA, Dobisz E, Kercher DS, et al. 2008. Density multiplication and improved lithography by directed block copolymer assembly. *Science* 321:936–39
139. Tada Y, Akasaka S, Yoshida H, Hasegawa H, Dobisz E, et al. 2008. Directed self-assembly of diblock copolymer thin films on chemically-patterned substrates for defect-free nano-patterning. *Macromolecules* 41:9267–76
140. Tada Y, Akasaka S, Takenaka M, Yoshida H, Ruiz R, et al. 2009. Nine-fold density multiplication of hcp lattice pattern by directed self-assembly of block copolymer. *Polymer* 50:4250–56
141. Xiao S, Yang X, Park S, Weller D, Russell TP. 2009. A novel approach to addressable 4 teradot/in.^{2} patterned media. *Adv. Mater.* 21:2516–19
142. Bita I, Yang JKW, Jung YS, Ross CA, Thomas EL, Berggren KK. 2008. Graphoepitaxy of self-assembled block copolymers on two-dimensional periodic patterned templates. *Science* 321:939–43
143. Stoykovich MP, Muller M, Kim SO, Solak HH, Edwards EW, et al. 2005. Directed assembly of block copolymer blends into nonregular device-oriented structures. *Science* 308:1442–46
144. Kang H, Craig GSW, Nealey PF. 2008. Directed assembly of asymmetric ternary block copolymer-homopolymer blends using symmetric block copolymer into checkerboard trimming chemical pattern. *J. Vac. Sci. Technol. B* 26:2495–99
145. Stoykovich MP, Kang H, Daoulas KC, Liu G, Liu C-C, et al. 2007. Directed self-assembly of block copolymers for nanolithography: fabrication of isolated features and essential integrated circuit geometries. *ACS Nano* 1:168–75
146. Wilmes GM, Durkee DA, Balsara NP, Liddle JA. 2006. Bending soft block copolymer nanostructures by lithographically directed assembly. *Macromolecules* 39:2435–37
147. Cheng JY, Rettner CT, Sanders DP, Kim H-C, Hinsberg WD. 2008. Dense self-assembly on sparse chemical patterns: rectifying and multiplying lithographic patterns using block copolymers. *Adv. Mater.* 20:3155–58

RELATED RESOURCES

Black CT, Ruiz R, Breyta G, Cheng JY, Colburn ME, et al. 2007. Polymer self assembly in semiconductor microelectronics. *IBM J. Res. Dev.* 51:605–33

Darling SB. 2007. Directing the self-assembly of block copolymers. *Prog. Polym. Sci.* 32:1152–204

Hamley IW. 2009. Ordering in thin films of block copolymers: fundamentals to potential applications. *Prog. Polym. Sci.* 34:1161–210

Kim H-C, Hinsberg WD. 2008. Surface patterns from block copolymer self-assembly. *J. Vac. Sci. Technol. A* 26:1369–82

van Zoelen W, ten Brinke G. 2008. Thin films of complexed block copolymers. *Soft Matter* 5:1568–82

Wang J-Y, Chen W, Russell TP. 2009. Patterning with block copolymers. In *Unconventional Nanopatterning Techniques and Applications*, ed. JA Rogers, HH Lee, pp. 233–89. Hoboken: Wiley

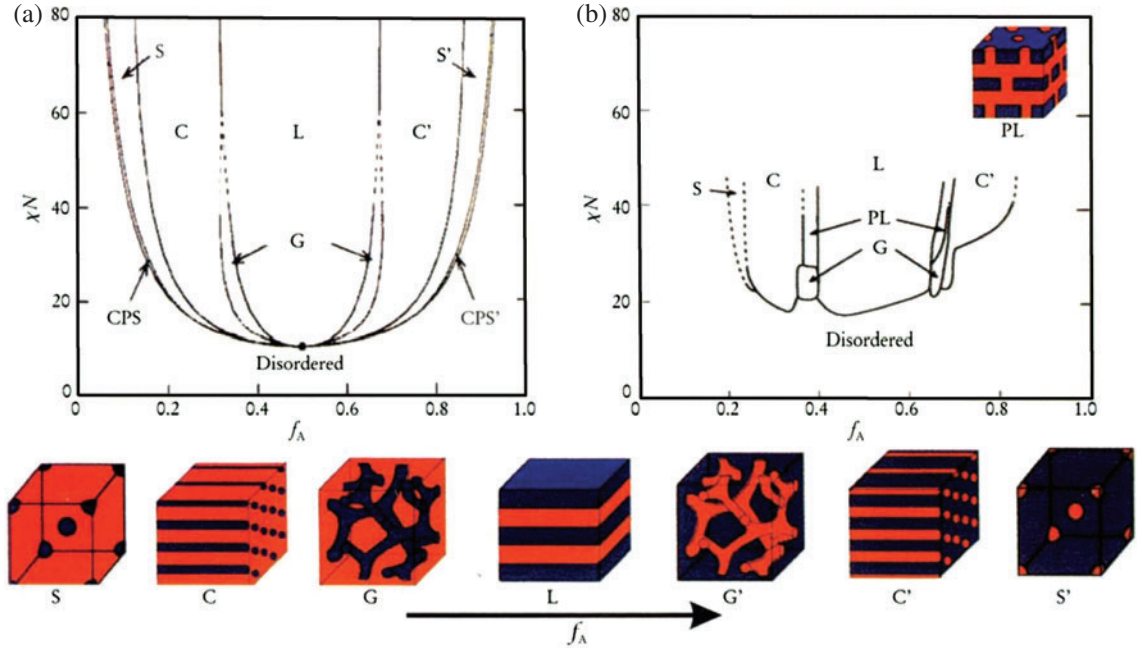

Figure 1

(*a*) Theoretical and (*b*) representative experimental phase diagram for linear A-*b*-B block copolymers as a function of the volume fraction of A block (f_A). Along the bottom of the figure are representations of four different equilibrium morphologies: S = body-centered-cubic spheres, C = cylinders, G = gyroid, and L = lamellae. Other structures found theoretically or experimentally include close-packed spheres (CPS) and perforated lamellae (PL). The characteristic spacing of the pattern of the structure, on the order of tens of nanometers, may be tuned through molecular weight. Reproduced with permission from Reference 22. Copyright © 1999, American Institute of Physics.

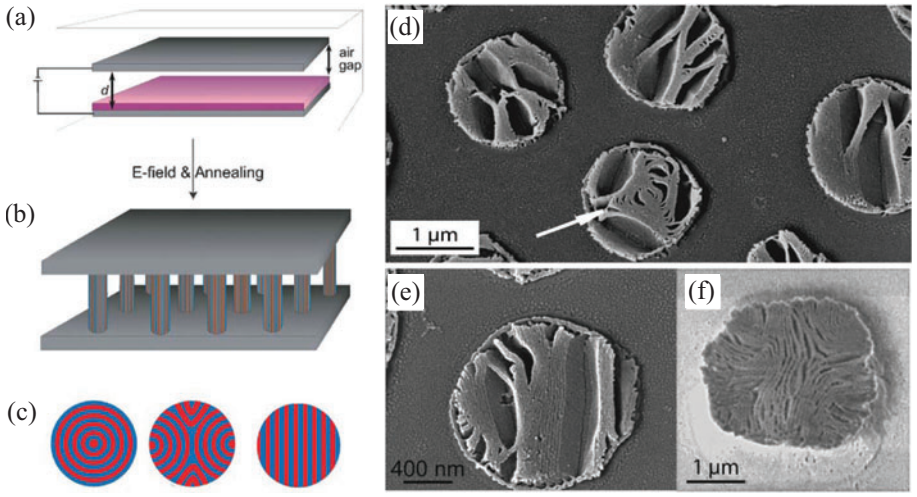

Figure 2

(*a*) A thin block copolymer film is placed on a substrate with a top electrode removed from the surface by an air gap. (*b*) During annealing, a voltage is applied between the electrodes, inducing flow of the block copolymer to form pillars. (*c*) The resulting flow orients the lamellae-forming poly(styrene-*b*-methyl methacrylate) (PS-*b*-PMMA) perpendicular to the substrate, though various in-plane orientations are possible. (*d*)–(*f*) Scanning electron micrographs of the oriented lamellae after exposure to UV light and rinsing with acetic acid to remove the PMMA blocks, revealing different in-plane orientations of the lamellae in different pillars. Reproduced with permission from Reference 70. Copyright © 2008, Wiley-VCH Verlag GmbH & Co. KGaA.

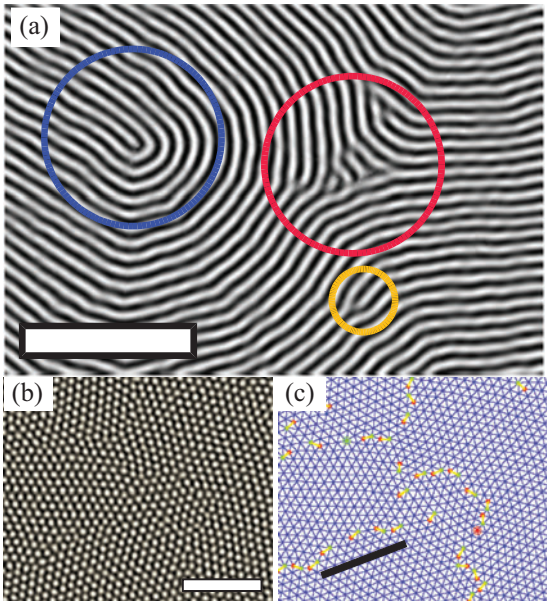

Figure 3

(*a*) Scanning electron micrograph of a cylinder-forming PS-*b*-poly(isoprene) (PS-*b*-PI) block copolymer thin film that showcases the defects possible in a 2D striped lattice (72). The blue circle shows a +1/2 disclination, the red circle shows a −1/2 disclination, and the orange circle shows a dislocation (scale bar = 400 nm). Reproduced with permission from Reference 72. Copyright © 2002, The American Physical Society. (*b*) Scanning electron micrograph of a sphere-forming PS-*b*-PI and (*c*) its corresponding Delaunay triangulation showcasing the defects possible in 2D hexagonal lattices (74). An isolated green dot is a sphere with seven nearest neighbors and corresponds to a −60° wedge disclination, whereas an isolated red dot has five nearest neighbors and corresponds to a +60° wedge disclination. Red and green dots connected by a yellow line form an edge dislocation (scale bar = 300 nm). Isolated dislocations retain the global orientation of the lattice whereas the disclinations destroy it. (*b*), (*c*) Reproduced with permission from Reference 74. Copyright © 2004, EDP Sciences.

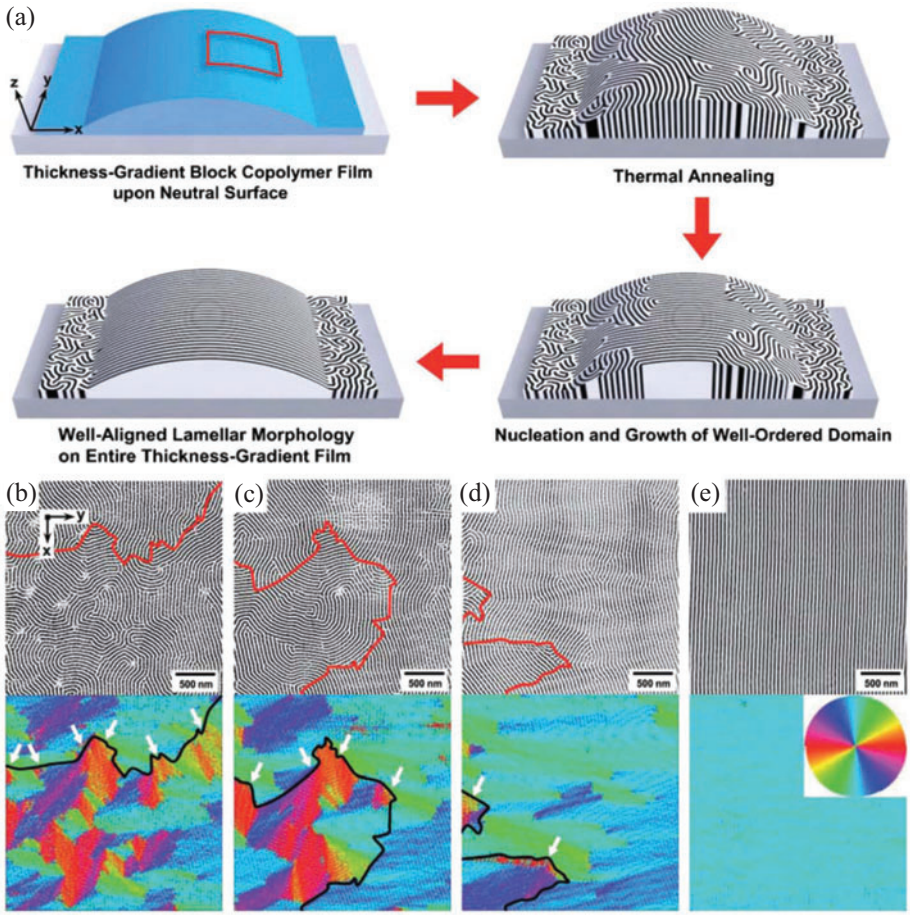

Figure 4

(*a*) Mechanism of lamellae alignment on a neutral surface that is driven by a thickness gradient. Grains nucleate in the thickest part of the film because of geometric anchoring, and then preferential movement of defects in the direction of the gradient aligns the rest of the block copolymer. (*b*)–(*e*) Atomic force micrographs (*top*) and corresponding false-color images (*bottom*) showing the in-plane orientation of lamellar interfaces in a PS-*b*-PMMA block copolymer annealed for 120, 150, 180, and 210 minutes, respectively, illustrating the movement of the grain boundary in the direction of the thickness gradient. Reproduced with permission from Reference 84. Copyright © 2009, Wiley-VCH Verlag GmbH & Co. KGaA.

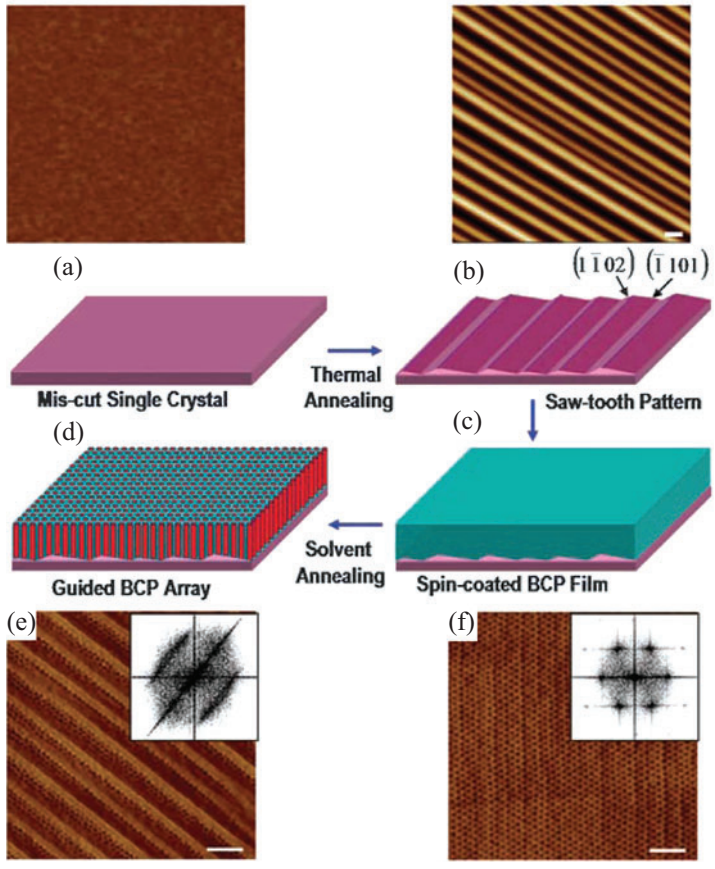

Figure 5

Schematic illustration of the use of faceted surfaces to orient cylinder-forming PS-*b*-poly(ethylene oxide) (PS-*b*-PEO). (*a*) The sapphire surface was mis-cut relative to a specific crystallographic plane and then (*b*) thermally annealed to reconstruct the surface. After (*c*) application of the block copolymer and (*d*) solvent annealing, atomic force micrographs of the block copolymer show excellent registry with the faceted surface for film thicknesses of (*e*) 24 nm and (*f*) 34 nm (scale bar = 200 nm). Reproduced with permission from Reference 87. Copyright © 2009, American Association for the Advancement of Science.

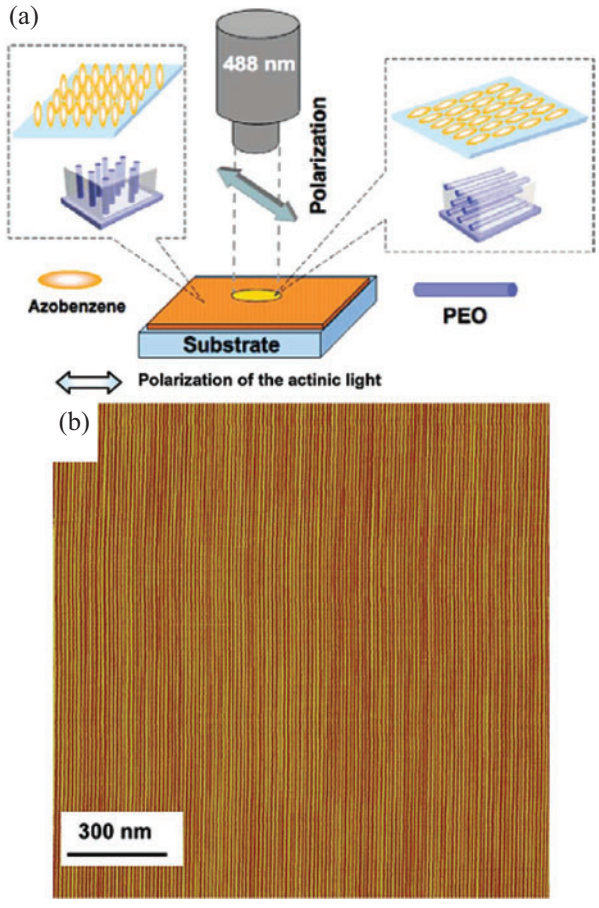

Figure 6

(*a*) Schematic representation of the use of polarized light to reorient the cylinders in PEO-*b*-poly(methacrylate-azobenzene) (PEO-*b*-PMA/AZ) block copolymer thin films from their initial configuration normal to the substrate to a new configuration parallel to the substrate and orthogonal to the polarization direction. (*b*) An atomic force micrograph of the highly aligned, defect-free cylinders oriented normal to the polarization direction. Reproduced with permission from Reference 101. Copyright © 2006, American Chemical Society.

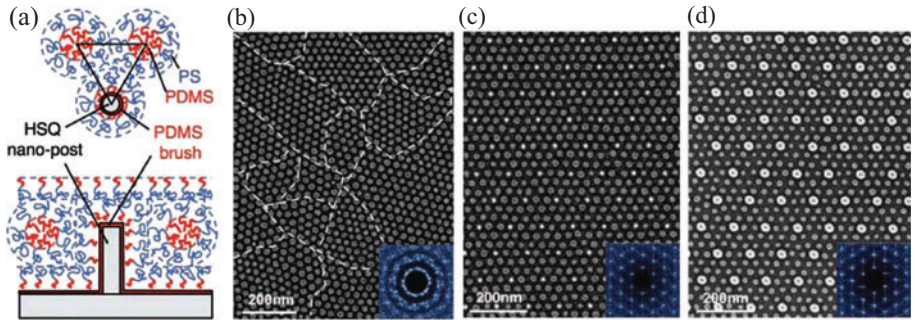

Figure 7

(*a*) Schematic representation of the polymer chain configuration around posts [fabricated from hydrogen silsesquioxane (HSQ)] wetted by the minority block of a sphere-forming PS-*b*-poly(dimethylsiloxane) (PS-*b*-PDMS) in thin films. (*b*) Scanning electron micrograph of polygranular structures of the block copolymer on an untemplated substrate and on a substrate with posts wetted by (*c*) the minority PDMS phase and (*d*) the majority PS phase. Appropriate size and functionalization of the posts leads to perfect orientational and positional control over the spherical phases. Reproduced with permission from Reference 142. Copyright © 2008, American Association for the Advancement of Science.

Annual Review of Chemical and Biomolecular Engineering

Volume 1, 2010

Contents

Errata

An online log of corrections to *Annual Review of Chemical and Biomolecular Engineering* articles may be found at http://chembioeng.annualreviews.org/errata.shtml